


Probabilistic Foot Contact Estimation by Fusing Information from Dynamics and Differential/Forward Kinematics

Conference Paper**Author(s):**

Hwangbo, Jemin; Bellicoso, Carmine D.; Fankhauser, Péter; [Hutter, Marco](#) 

Publication date:

2016

Permanent link:

<https://doi.org/10.3929/ethz-a-010711905>

Rights / license:

[In Copyright - Non-Commercial Use Permitted](#)

Originally published in:

<https://doi.org/10.1109/IROS.2016.7759570>

Probabilistic Foot Contact Estimation by Fusing Information from Dynamics and Differential/Forward Kinematics

Jemin Hwangbo^{†,1}, Carmine Dario Bellicoso[†], Péter Fankhauser^{*} and Marco Hutter[†]

Abstract—Legged robots require a robust and fast responding feet contact detection strategy. Common force sensors are often too heavy and can be easily damaged during impacts with the terrain. Therefore, it is desirable to detect a contact without a force sensor. This paper introduces a probabilistic contact detection strategy which considers full dynamics and differential/forward kinematics to maximize the use of available information for contact estimation. This paper shows that such strategy is much more accurate than the state-of-the-art strategy that only take one measure into account, with a quadrupedal robot.

I. INTRODUCTION

To control legged robots, feet contact state with the terrain has to be reliably estimated since the dynamics of legged robots highly depends on contact forces acting on the feet. Typically, this has been done with force sensors which can directly measure the contact forces. Thresholding the force values gives a simple contact state classifier.

In case of dynamic robots like StarLETH [1] and its decedent ANYmal [2], adding force sensors at the feet is undesirable due to the following three reasons. First, due to their high speed motions and impacts at the feet, the sensors are likely to be damaged over a repeated use. A contact detection strategy relying only on force sensors might lead to a catastrophic damage to the robot when the sensors are malfunctioning. Second, the sensors and their protection shells contributes significant portion of the overall leg inertia. Although it can be underestimated, a 100 g sensor at the foot contributes about 50 % of the overall leg inertia for robots like StarLETH. High leg inertia leads to high impact losses at touch-down events and low acceleration capability of the leg. Third, robust and reliable 3D force sensors are expensive and rare. These sensors contribute significant portion of the cost of the robot and make the existing robots less affordable.

Sensorless ground contact estimation has been rarely investigated in the context of legged robots. Hyun et. al. briefly explain their approach in [3]. They measure position tracking error during swing phase and threshold this value to classify the foot contact. This method does not consider the dynamics of the swing leg and, therefore, is not accurate when the leg is swinging fast. Focchi et. al. identify the contact using estimated ground reaction forces acting on the foot [4]. This approach is in fact unfiltered version of Generalized Momentum (GM) based approaches presented in [5], [6].

A GM-based approach is equivalent to low pass filtering the estimated force at the foot and threshold it to identify a collision.

Note that there is a slight difference between the previous *collision* detection strategies and a *contact* detection that is presented in this paper. Collision detection strategies aim to detect an impact whereas contact detection strategies aim to detect accurate timing of the loss of the contact as well.

A. Overview of the Method

The proposed method considers all measurements related to the dynamics and differential/forward kinematics of the robot. The information in the dynamics is abnormalities in acceleration. If the estimated acceleration of the foot is high, it is likely that the foot is freely moving in the air. Information from the differential kinematics is useful when the foot is moving at high speed. High foot velocity means that the foot is not likely to be in contact with the terrain. Fusing this information improves the detection capability during swing phase where the noise, which comes from modeling errors, inaccurate calibration and torque noises, is significant in dynamics. Estimation from forward kinematics further improves the quality of the contact detection. Intuitively, when a foot is high off the ground, it is not likely be in contact with the ground. When the terrain model is known, this kinematic information improves the detection capability significantly. Even if the terrain model is not known, the distribution of the terrain can be conservatively estimated with an assumption on the roughness of the terrain. In other words, a certain variance in the ground height can be assumed if a foot is placed close to where it WAS placed before. Another use of forward kinematics is in a transition model. When high upward velocity is detected in the air, it is very unlikely that the foot contacts the ground. When high upward velocity is detected on the ground, the foot probably has lost its contact.

The paper introduces a probabilistic approach for foot contact state estimation. It includes a full probabilistic model, consisting of a transition model and a measurement model, to fuse dynamics and forward/differential kinematics information together. This paper specifically illustrates in detail the modeling method for detecting a contact between a foot and a terrain but it can be simplified/modified to be used in a general contact detection scenario as well. An implementation on a quadruped robot and comparison to the state-of-the-art approaches are presented in this paper.

*This research was supported by the Swiss National Science Foundation through the National Centre of Competence in Research Robotics.

¹jhwangbo@ethz.ch

[†]Robotic Systems Lab (RSL), ETH Zurich, Switzerland

^{*}Autonomous Systems Lab (ASL), ETH Zurich, Switzerland

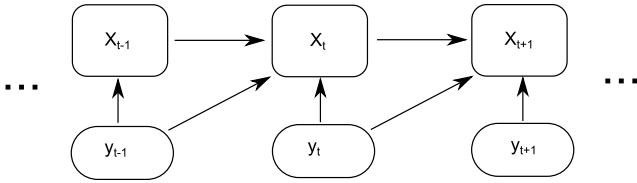


Fig. 1: A probabilistic graphical model of the contact state.

II. MODELING

The objective is to identify the binary foot contact state $X_t \in \{N, F\}$, where N and F represent ‘on the terrain’ and ‘off the terrain’, respectively. Individual foot states are modeled separately to reduce the complexity of the problem. The graphical probabilistic model is shown in Fig. 1. It is assumed that Markov assumption holds in the system which means that the contact state probability distribution is independent of the previous states given the state at the current time step. The state of the robot is represented by the generalized coordinate \mathbf{q} and the generalized velocities $\dot{\mathbf{q}}$ which can be obtained from a state estimation system that fuses information from an Inertial Measurement Unit (IMU) and joint encoders [7]. The proposed method currently uses loosely coupled contact and state estimation approaches so that the contact estimation strategy can be stand-alone. The additive noises \mathbf{w}_q , $\mathbf{w}_{\dot{q}}$ and $\mathbf{w}_{\ddot{q}}$ are assumed to be uncorrelated since the estimates are filtered at very different cutoff frequencies. This implies that the position updates occur at a high frequency such that the joint acceleration can be estimated at a reasonably high frequency. However, this paper shows that the contact state can be accurately estimated even with a noisy acceleration measurement with real robotic examples.

The transition probability is dependent on the measurements since the feet velocity is crucial in estimating the transition. Since the objective of this work is to estimate the probability of the current contact state only, the following iterative algorithm, which is in fact equivalent to the *forward algorithm* of Hidden Markov Model (HMM), is introduced:

$$\alpha(X_t) = P(X_t, \hat{\mathbf{q}}_{1:t}, \hat{\dot{\mathbf{q}}}_{1:t}, \hat{\ddot{\mathbf{q}}}_{1:t}, \zeta) = \underbrace{P(\hat{\mathbf{q}}_t, \hat{\dot{\mathbf{q}}}_t, \hat{\ddot{\mathbf{q}}}_t | X_t)}_{\text{measurement model}} \cdot \sum_{X_{t-1}} \underbrace{P(X_t | X_{t-1}, \hat{\mathbf{q}}_{t-1}, \hat{\dot{\mathbf{q}}}_{t-1}, \hat{\ddot{\mathbf{q}}}_{t-1}, \zeta)}_{\text{transition model}} \alpha(X_{t-1}), \quad (1)$$

where ζ is a behavioral pattern of the robot that contains information about the state transition probability. In the case of legged robots, it is defined by a gait pattern. Note that the estimates are independent of ζ given the corresponding state and that is why it is omitted in the measurement model. The commonly accepted notations $\mathbf{q}_t = \mathbf{q}(t)$ and $\mathbf{q}_{1:t} = \{\mathbf{q}_1, \mathbf{q}_2, \dots, \mathbf{q}_t\}$ are used throughout this paper. Since the transition model is dependent on the measurement as well, the system cannot be modeled as a HMM but it is highly related. After obtaining $\alpha(X_t)$, the probability of the contact state can be obtained from the definition of

conditional probability as

$$P(X_t = S | \hat{\mathbf{q}}_{1:t}, \hat{\dot{\mathbf{q}}}_{1:t}, \hat{\ddot{\mathbf{q}}}_{1:t}, \zeta) = \frac{\alpha(X_t = S)}{\sum_{\forall X_t} \alpha(X_t)}, \quad (2)$$

where S is the value of the contact state which can be either F or N .

A. Measurement Model

The measurement model can be extended as

$$P(\hat{\mathbf{q}}_t, \hat{\dot{\mathbf{q}}}_t, \hat{\ddot{\mathbf{q}}}_t | X_t) = \underbrace{P(\hat{\mathbf{q}}_t | X_t, \hat{\mathbf{q}}_t, \hat{\dot{\mathbf{q}}}_t)}_{\text{dynamics}} \underbrace{P(\hat{\dot{\mathbf{q}}}_t | X_t, \hat{\mathbf{q}}_t)}_{\text{differential kinematics}} \underbrace{P(\hat{\ddot{\mathbf{q}}}_t | X_t)}_{\text{kinematics}}. \quad (3)$$

Each term represents dynamics, differential kinematics and kinematics respectively. The following subsections illustrate the method of calculating each term.

1) *Dynamics*: Only the dynamics of a leg is considered at a time since external forces on the main body can ruin the estimation. Using the state estimation system, dynamics of the main body can be replaced by measurements and estimation. The leg then can be modeled as a constrained multi-body system in a non-inertial reference frame. The equation of motion can be written as

$$\mathbf{M}_l(\mathbf{q}_l(t))\ddot{\mathbf{q}}_l(t) + \mathbf{M}_{lb}(\mathbf{q}_l(t))\ddot{\mathbf{q}}_b(t) + \mathbf{h}_l(\mathbf{q}_{lb}(t), \dot{\mathbf{q}}_{lb}(t)) + \mathbf{J}_{fl}^T(\mathbf{q}_{lb}(t))\mathbf{F}_f(t) = \mathbf{S}^T\boldsymbol{\tau}(t), \quad (4)$$

where \mathbf{q}_l , \mathbf{q}_b and \mathbf{q}_{lb} represent generalized coordinate of a leg, the base frame and the concatenation of the two, \mathbf{M}_l and \mathbf{M}_{lb} represent inertia matrix of the leg and the coupling matrix between the two generalized coordinates, \mathbf{h}_l is the non-linear terms including coriolis and gravity, $\boldsymbol{\tau}$ is the actuation torques, \mathbf{S}^T is the torque selection matrix that maps actuation torques to the equivalent generalized forces, \mathbf{J}_f is the contact Jacobian, \mathbf{J}_{fl} is the block of \mathbf{J}_f that is responsible for the leg coordinate and \mathbf{F}_f is the contact force. From here on, the arguments like t and \mathbf{q} will be dropped whenever there is no confusion in interpretation. We can rearrange the equation to

$$\ddot{\mathbf{q}}_l = \mathbf{M}_l^{-1}(\mathbf{S}^T\boldsymbol{\tau} - \mathbf{M}_{lb}\ddot{\mathbf{q}}_b - \mathbf{h}_l - \mathbf{J}_{fl}^T\mathbf{F}_f). \quad (5)$$

If there is no contact, the contact force is zero. If there is a contact, the estimated contact force can be written as a function of the joint torque as

$$\hat{\mathbf{F}}_f = (\mathbf{J}_{fl}\mathbf{M}_l^{-1}\mathbf{J}_{fl}^T)^{-1} \left\{ \mathbf{J}_f \left[\mathbf{M}_l^{-1}(\mathbf{S}^T\boldsymbol{\tau} - \mathbf{M}_{lb}\ddot{\mathbf{q}}_b - \mathbf{h}_l) \right] + \dot{\mathbf{J}}_f\dot{\mathbf{q}}_{lb} \right\}. \quad (6)$$

There are many sources of errors due to model uncertainties and disturbances. For practical reasons, only the error in the acceleration measurement, the error due to external forces/torques and the error due to the slippages at the contact are considered. Then the measurement model can be written as

$$\hat{\mathbf{q}}_l = \mathbf{M}_l^{-1}(\hat{\mathbf{q}}_l) \{ \mathbf{S}^T\boldsymbol{\tau} - \mathbf{M}_{lb}(\hat{\mathbf{q}}_l)\hat{\ddot{\mathbf{q}}}_b - \mathbf{h}_l(\hat{\mathbf{q}}_{lb}, \hat{\dot{\mathbf{q}}}_{lb}) - \mathbf{J}_{fl}^T(\hat{\mathbf{q}}_{lb})\mathbf{F}_f(\hat{\mathbf{q}}_{lb}, \hat{\dot{\mathbf{q}}}_{lb}) + \mathbf{w}_d + \mathbf{J}_{fl}^T(\hat{\mathbf{q}}_{lb})\mathbf{w}_f \} + \mathbf{w}_{\ddot{q}}, \quad (7)$$

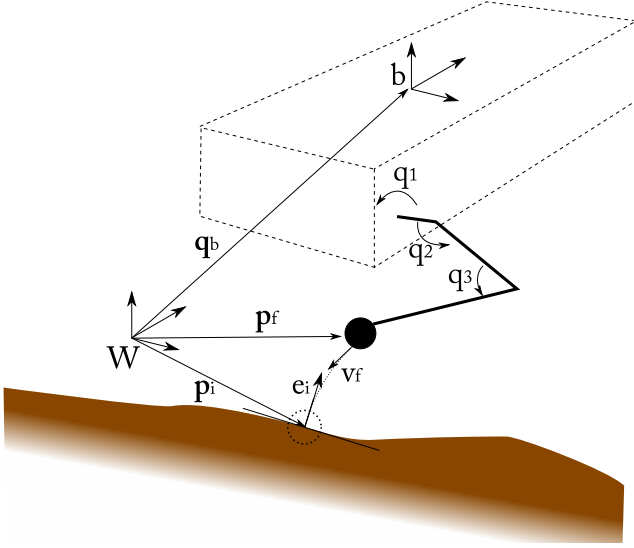


Fig. 2: Probabilistic Graphical Model of contact state.

where w_f is the noise from the contact force estimate, w_q is the estimation noise in acceleration and w_d is the combined noise from all other sources including the possible modeling errors and external disturbances. All the errors are assumed to be Gaussian distributed in this work. If a foot slippage occurs regularly, then the variance in the foot force in horizontal direction should be increased or the foot Jacobian should be simplified to z-row only. It is practically impossible to measure all the noises accurately. So the covariance of w_d has to be tuned wherever it is necessary.

Note that there is a fundamental difference between the proposed contact detection and the existing works on collision detection. When there is zero contact force, there is no collision but there might be a contact. This paper deals with a contact estimation for control.

2) *Differential Kinematics*: The measurement model for the generalized velocity when the foot is in the air is given as

$$\hat{\dot{q}} = \dot{q} + w_q. \quad (8)$$

The distribution of \dot{q} has to be estimated from data in theory. Alternatively, it can be approximated knowing that \dot{q} lives in the null space of the contact constraint Jacobian. Therefore, the following measurement model is proposed:

$$\hat{\dot{q}} = \{I - J_f^+(\hat{q})J_f(\hat{q})\}\dot{q} + w_q + w_J, \quad (9)$$

where w_J is the artificial noise that is added to compensate for the errors due to the Jacobian term and w_q is the noise in the velocity measurement. The term \dot{q} in this equation represents the prior distribution of the generalized velocity which can be either measured or estimated using the velocity limits. Note that all the distributions are assumed to be Gaussian distributed for convenience.

3) *Kinematics*: The proposed method also requires the terrain information to estimate the probability of a contact. The proposed method assumes that some type of terrain information is given with its uncertainty; it can be a height

map from a mapping algorithm, terrain estimation using Gaussian Process (GP) regression from previous foot steps or a simple flat terrain assumption with a high variance. In this work, a flat terrain model is used with a high uncertainty due to the lack of a mapping algorithm.

The contact probability depends on the kinematics at time t . The kinematics regarding the contact can be described with two vectors: position of the foot p_f and the position of the impact point p_i . Assuming that the ground is relatively smooth, 1D coordinate frame called *impact frame* is introduced. Impact frame originates at the impact point and its axis points to the opposite direction of the velocity of the foot at the impact as shown in Fig. 2. If the impact point is not planned in prior, it has to be assumed with the current velocity. The unit vector along the axis of the impact frame expressed in the world frame is denoted as e_i . The projections of p_f and p_i to the space spanned by e_i are denoted as p_f and p_i respectively. These projected variables have certain distributions along the impact axis. The distribution of p_i can be either obtained from mapping algorithms or estimated conservatively. The distribution of p_f is simple to obtain since the state estimation algorithm estimates the states as a Gaussian distribution which can be mapped to the cartesian coordinates of the foot using the foot Jacobian.

For a concise expression, a gap function

$$\phi(t) = p_f - p_i \quad (10)$$

is introduced. Negative gap means that the contact is closed. The probability of such event can be obtained from the cumulative distribution $P_\phi(0) = \int_{-\infty}^0 P_\phi(s)ds$.

B. Transition Model

The transition probability can be obtained from the linearized model $q_t = q_{t-1} + \Delta t \dot{q}_{t-1}$ where Δt is the time step between $t-1$ and t . The distribution of v_f , which is the velocity of the foot v_f projected to the impact axis, is defined similarly to p_f in section II-A.3.

It is convenient to separate the transition model into two cases: $X_{t-1} = F$ and $X_{t-1} = N$. The following two sections deal with the transition model at each case.

1) *Transition from contact*: The estimates are independent of ζ given their corresponding states. Using Bayes' theorem, the transition probability can be extended as

$$\begin{aligned} P(X_t|X_{t-1}, \hat{q}_{t-1}, \hat{q}_{t-1}, \hat{q}_{t-1}, \zeta) &= \\ &= \frac{P(\hat{q}_{t-1}, \hat{q}_{t-1}, \hat{q}_{t-1}|X_t, X_{t-1})P(X_t|X_{t-1}, \zeta)}{\sum_{X_t} \underbrace{P(\hat{q}_{t-1}, \hat{q}_{t-1}, \hat{q}_{t-1}|X_t, X_{t-1})}_{\text{forward kinematics}} \underbrace{P(X_t|X_{t-1}, \zeta)}_{\text{prior}}} \end{aligned} \quad (11)$$

The prior probability $P(X_t|X_{t-1}, \zeta)$ can be obtained from gait pattern ζ . Given the average stance duration T_s ,

$$\begin{aligned} P(X_t = F|X_{t-1} = N, \zeta) &= \Delta t/T_s \text{ and} \\ P(X_t = N|X_{t-1} = N, \zeta) &= 1 - \Delta t/T_s. \end{aligned} \quad (12)$$

Algorithm 1 Approximating the impact probability**initialize** $\alpha = 0$ **for** predefined number of samples n_s Sample p_f from $\mathcal{N}(\bar{p}_f, \sigma_{p_f})$ Sample p_i from $P(p_i|p_f) = \begin{cases} \frac{\mathcal{N}(\hat{p}_i, \sigma_{p_i})}{F(p_f, \hat{p}_i, \sigma_{p_i})}, & \text{if } p_f \leq p_i \\ 0, & \text{if } p_f > p_i \end{cases}$ $\alpha = \alpha + F((p_f - p_i)/\Delta t, \bar{v}_f, \sigma_{v_f})$ **end for** $P(\phi(t+1) < 0) = \alpha/n_s;$

The term $P(\hat{\mathbf{q}}_{t-1}, \hat{\mathbf{q}}_{t-1}, \hat{\mathbf{q}}_{t-1}|X_t, X_{t-1} = N)$ is trivial for the case $X_t = N$ since $v_f = \mathbf{e}_i^T \mathbf{J}_f \dot{\mathbf{q}} = 0$. The measurement model is

$$\hat{v}_f = w_v \quad (13)$$

where w_v is containing all the estimation errors projected to the impact frame. Again this has to be conservatively estimated to account for modeling errors. Given $X_t = F$, the measurement model can be written as

$$\hat{v}_f = v_f + w_v. \quad (14)$$

Note that assuming $v_f(t-1) = 0$ is not feasible since the foot will never take-off. Here the assumption $v_f(t-2) = 0$ is made following the linearized model. Therefore, the foot can have a finite velocity even on the terrain if it takes off at the next time step. The distribution $P(v_f|X_t = F, X_{t-1} = N)$ can be obtained from experiments. For convenience, it is assumed to be a uniform distribution defined as $U(0, \mathbf{e}_i^T \mathbf{J}_f(\hat{\mathbf{q}})\ddot{\mathbf{q}}_F \Delta t)$, where $\ddot{\mathbf{q}}_F$ is the max acceleration commanded for a take-off. Assuming it to be a uniform distribution leads to the following analytical solution:

$$P(v_f|X_t = F, X_{t-1} = N) = F(v_f(t-1), v_f(t-1) - \mathbf{e}_i^T \mathbf{J}_f(\hat{\mathbf{q}})\ddot{\mathbf{q}}_F \Delta t, 0, \sigma_{v_f}), \quad (15)$$

where $F(x_1, x_2, \mu, \sigma)$ is the probability integrated from x_1 to x_2 in a normal distribution function with a mean of μ and a standard deviation of σ . If the function has only three arguments, it represents the common cumulative distribution function.

2) *Transition in the air:* In this case, the probability $P(X_t|X_{t-1}, \hat{\mathbf{q}}_t, \hat{\mathbf{q}}_t, \hat{\mathbf{q}}_t)$ can be directly evaluated. This term is a probability of an impact given the foot position, velocity and terrain measurements. Again, a gap function is employed as

$$\phi(t) = p_f + \Delta t v_f - p_i. \quad (16)$$

$\phi(t+1) < 0$ with $X_{t-1} = F$ implies that the foot strikes the ground. There are two noticeable properties of the distributions of p_f , v_f and p_i given $X_{t-1} = F$:

- There is no collision if $v_f > 0$ and
- $P(p_i > p_f|X_t = F) = 0$.

In other words, the foot cannot strike the ground if it is moving away from the ground and the ground is always below the foot. Therefore, p_f , v_f and p_i cannot be assumed

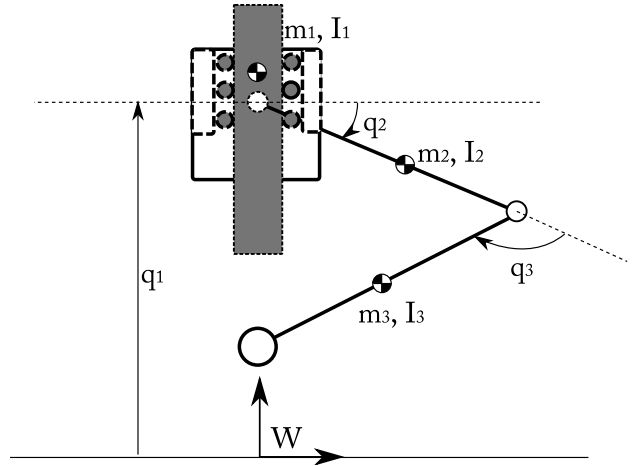


Fig. 3: Probabilistic Graphical Model of contact state.

to be Gaussian distributed. The following distribution model is proposed:

$$\begin{aligned} p_f &\sim \mathcal{N}(\mu_{p_f}, \sigma_{p_f}) \\ v_f &\sim \mathcal{N}(\mu_{v_f}, \sigma_{v_f}) \\ P(p_i|p_f) &= \begin{cases} \frac{\mathcal{N}(\hat{p}_i, \sigma_{p_i})}{F(p_f, \hat{p}_i, \sigma_{p_i})}, & \text{if } p_f \leq p_i \\ 0, & \text{if } p_f > p_i. \end{cases} \end{aligned} \quad (17)$$

This problem does not have an analytical solution so a sampling-based method such as Monte-Carlo methods should be used. A pseudo-code of an example method is given in algorithm 1. The computation time of such sampling method was less than $100 \mu s$ in MATLAB with 500 samples.

III. SIMULATION EXAMPLE

In this section, a simple 2D example is introduced to demonstrate the proposed method. The base is fixed to a 1D rail and the two leg components, the thigh and the shank, are attached to their previous link by a rotary joint as shown in Fig. 3. The model parameters are listed in Tab. I. The

TABLE I: Model Parameters

Parameter name	value
m_1	5.449 kg
m_2, I_2, r_2	2.48 kg, $3.18 \times 10^{-2} \text{kgm}^2$, 0.043 m
m_3, I_3, r_3	0.31 kg, $1.383 \times 10^{-2} \text{kgm}^2$, 0.039 m
max torque	30 Nm
max joint speed	25 rad/s

characteristics of these noises are assumed to be available for the estimation. The actual measurements used for the estimation are shown in Fig. 4 Note that the noise in all the measurements are extremely high. Figure 5 shows the fused estimate, the measurement model probabilities and the transition probabilities. The fused estimate of the contact is clean except the small delay in estimating the first take off.

Each measurement is effective at different stages. The dynamic measurement model is reliable¹ when the foot is

¹here the reliability means that the probability is close to either 0 or 1.

TABLE II: Noise Characteristics

noise	standard deviation
$w_{\ddot{q}}$	2 m/s ² , 100 rad/s ² , 100 rad/s ²
$w_{\dot{q}}$	0.2 m/s, 0.3 rad/s, 0.3 rad/s
w_q	0.04 m, 0.02 rad, 0.02 rad
w_d	1 N, 2 Nm, 2 Nm
w_f	F_f
w_{pf}	$(e^i)^T J^T F_f J e^i$
w_v	$(e^i)^T J \dot{q} J^T e^i$
w_{pi}	0.2 m

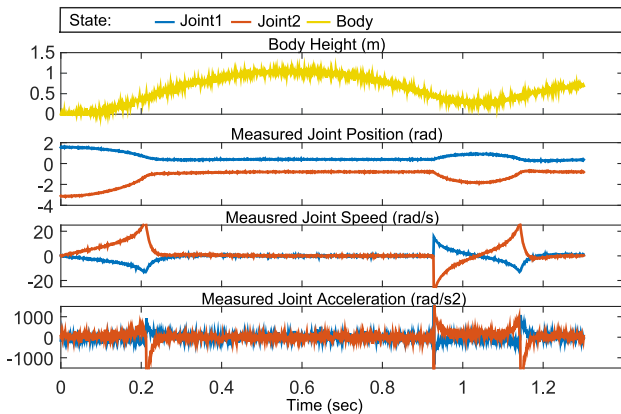


Fig. 4: Joint state/acceleration measurements.

in contact with the ground since high contact force is easily noticeable. The differential kinematic measurement model is reliable when the foot is moving fast in the swing phase and the kinematic measurement model is reliable when the foot is near its apex height. The differential kinematic measurement model is unreliable when the foot velocity is zero at the apex.

Each transition probability has its own effective region as well. The transition probability from contact to air is reliable when the foot lifts off and when it is about to touch down. The transition probability from air to contact only peaks up near the touch down phase when the foot is approaching the ground with high negative velocity. Consequently, when all the information is fused, the estimate of the contact becomes very reliable at every stage.

IV. VALIDATION ON A QUADRUPEDAL ROBOT

In this section, the contact estimation capability of the proposed method is demonstrated on a quadrupedal robot ANYmal [2]. ANYmal, shown in Fig. 6, is an electrically-driven quadrupedal robot whose weight is about 25 kg (before adding the extra sensor set) and the total leg length is about 50 cm. It is equipped with 12 torque-controllable Series Elastic Actuators (SEA) [8]. The spring in the SEA unit protects its gear upon impacts and offers a high quality joint torque measurement which is very useful for the contact estimation.

The position and velocity measurements are updated at 400 Hz from the actuator modules but the joint acceleration has to be calculated by differentiating the joint velocity externally due to the current limitations in hardware. The

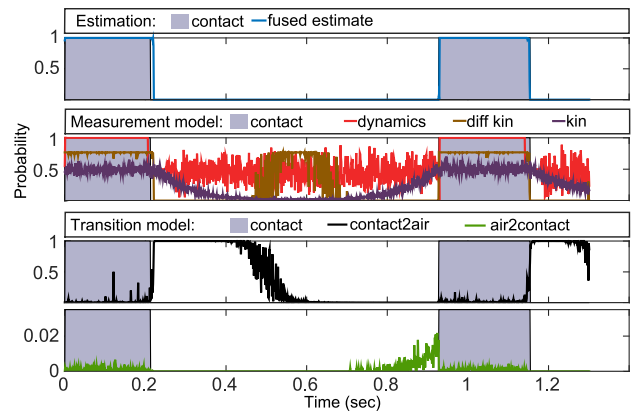


Fig. 5: Fused estimation on the foot contact (top), measurement model probabilities (2nd from top), and the transition probability (bottom two)



Fig. 6: Fused estimation on the foot contact (top), measurement model probabilities (2nd from top), and the transition probability (bottom two)

dynamic/kinematic parameters were identified with a scale and the CAD model. The feet are equipped with small force sensors² (≈ 100 g without a protection shell) that serve as a ground truth in the following experiments. The force sensors contribute about one third of the total leg inertia when the leg is fully stretched even without the protection shell. They highly limit the acceleration capability of ANYmal during a swing phase.

The proposed method is compared to the GM-based method for the two tasks presented in this section. GM-based contact classification is a simpler method which uses the dynamic information only. However, it is still the most related and well-recognized work so the result from this approach is presented as well for a comparison.

In a real robotic experiment, the measurements and the estimates are no longer normally distributed but rather correlated and biased. Therefore, the covariances of the noises are assumed to be high to account for these modeling errors. In addition, there is external disturbances that corrupt the measurements even though the robot was not perturbed

²Optoforce, <<http://optoforce.com/>>

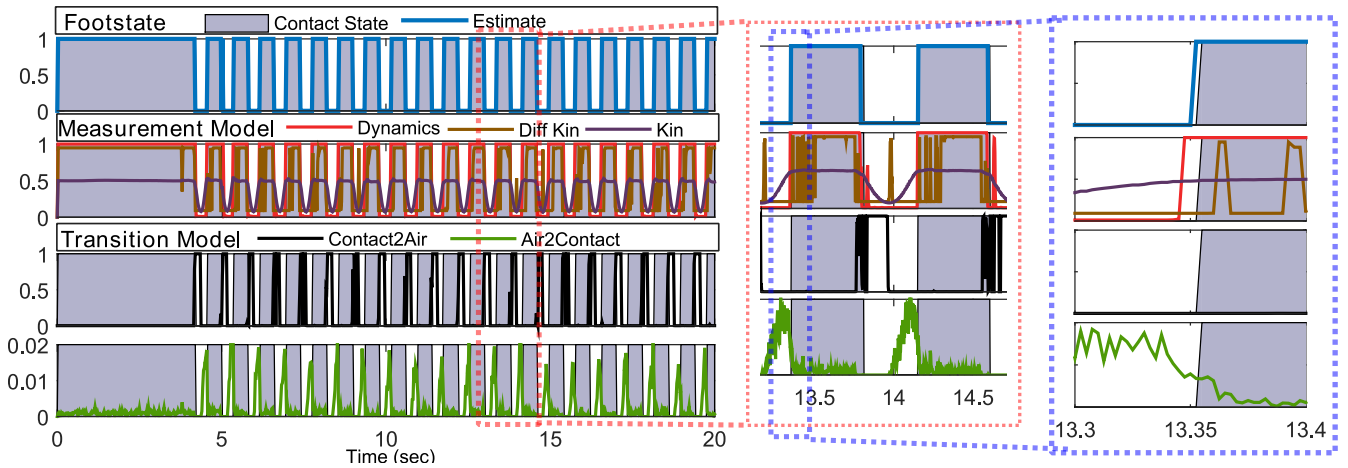


Fig. 7: Fused estimation on the foot contact (top), measurement model probabilities (2nd from top), and the transition probability (bottom two) from trotting Experiment with ANYmal.

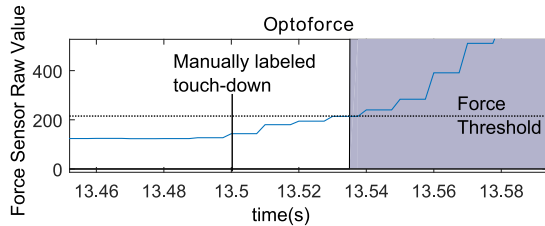


Fig. 8: Raw measurement from the force sensor.

explicitly for this experiment. The major error source is from the deviation from the rigid body assumption on the main body since not all components are rigidly mounted. This effect should be reflected in w_d .

The performance of the proposed strategy was evaluated by measuring the delay in the contact estimation for both experiments. To this end, the raw force sensor value was used to manually label the contact timing. Figure 8 shows the raw force value and the threshold used to identify a contact. Only the touch-down events are considered in the evaluation since the take-off timing could not be estimated accurately due to the hysteresis effect of the force sensor.

The first experiment was performed for about 20 sec with trotting gait. In trotting gait, the diagonal pairs of legs are contacting the ground at the same time. This gait is characterized by relatively high impacts at the feet at touch-down events compared to walking gaits.

The fused estimate, likelihood, and the transition probabilities are shown in Fig. 7 and the delays in the estimate are shown in Tab. III. Note that there were outliers in the velocity measurement so that the probabilities in the differential measurement model was limited to 90%. The general trend is the same as in the simulation. The contact estimate was visually flawless for all steps. The probabilistic estimate detects both touch-down and take-off little bit earlier than the force sensor. We believe that this is due to the delayed response in estimation using the force sensor. The late touch-down is due to the the compliance at the feet and

the force threshold that is used for contact identification. The late take-off detection is due to the hysteresis effect of the force sensor which was visible on the raw force reading. This contact detection delay for both take-off and touch-down was around 15 ms for trotting and around 25 ms for walking.

It is clear that the dynamic measurement only will cause noisy estimation near take-off. However, the contact-to-air transition probability was close to 1 which suppresses the noisy estimate from dynamic model. This confirms that the dynamic model only cannot have the same performance as the fully fused estimate.

The second experiment was carried out with slow walking gait on the terrain shown in Fig 9. To investigate the robustness of the proposed method, two modifications were made on the robot. First, an additional weight was placed on the mainbody to change the weight of the robot by about 3.0 kg. Second, a 200 g weight was mounted on a shank. The weight added to the shank translates to about 60% change in the shank inertia. The model for the contact estimation was not updated to reflect these changes. The contact estimator was tested with the left foreleg, which has the added mass, and the right foreleg, which does not have an added mass. The fused estimate, likelihood, and the transition probabilities for the left foreleg is shown in Fig. 10 and the delays in the estimate are shown in Tab. III.

	Trotting	Walking	Walking with added mass
Prob. based	6.03 ±4.51	19.69 ±3.39	43.214 ±9.21
GM-based, tuned for walking	4.134 ±3.24 (6 fail)	35.62 ±9.23 (1 fail)	46.07 ±5.74
GM-based, tuned for trotting	8.33 ±5.06 (1 fail)	59 ±16 .34	82.86 ±4.88

TABLE III: Average delay (in ms) in contact detection from the proposed strategy and the GM-based strategy.

The failure here is defined as a false contact detection in the air phase. This is generally caused by the inertial noise during the swing phase and the inaccurate model. Both strategies did not fail to detect contact during contact phase.

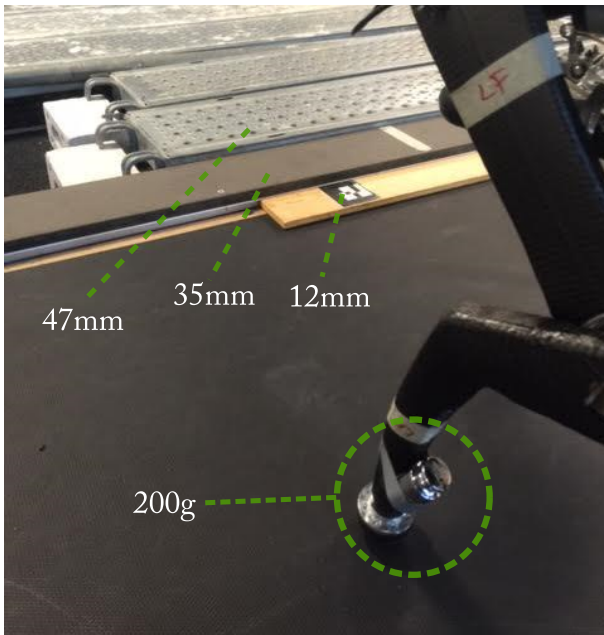


Fig. 9: The terrain height variations and the added mass for rough terrain walking experiment.

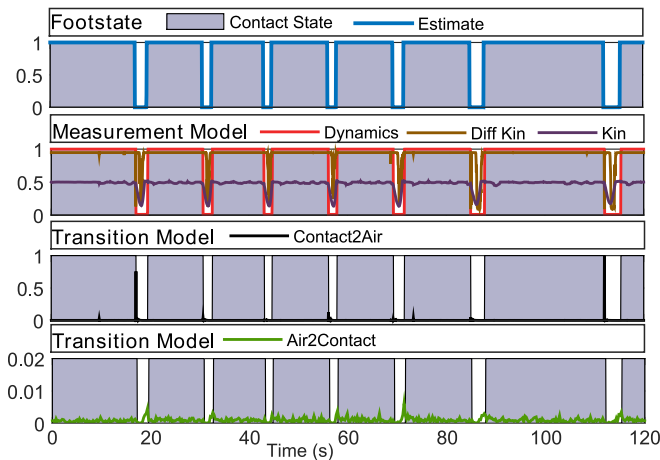


Fig. 10: Fused estimation on the foot contact (top), measurement model probabilities (2nd from top), and the transition probability (bottom two) from rough terrain walking experiment with ANYmal. The estimation heavily relies on the information from dynamics for slow gait.

However, due to the added mass at the shank, the contact detection was delayed for both strategies for walking gait as shown in Tab. III.

The GM-based strategy has two parameters to tune. To fairly compare the two strategies, the decaying factor K_I and the threshold were tuned such that the signal appears to be most reliable for each task. Note that in a real application, the threshold should be set for the most dynamic gait in order to avoid a false detection.

The result indicates that the proposed strategy is more reliable than the GM-based strategy. The GM-based strategy is in fact similar to the dynamic measurement model. It can also be interpreted that it has constant transition probabilities without considering the kinematics. This results in slow

response in detection. The proposed strategy also uses the velocity of the foot to calculate the touch-down probability which makes the proposed strategy more fast responding. The proposed method seems to be robust against a model error as well. A significant change in the inertia only caused 40 ms of additional delay. Since the controller is running at 400 Hz, it only delays the contact flag switch by 2 loops.

The proposed strategy was more reliable even with the noisy torque measurement. GM-based strategy failed 6 times if the threshold is lowered for fast contact detection. In the proposed strategy, the noisy dynamic prediction during swing phase was compensated by the differential dynamic estimate. Thanks to this information fusion, the proposed method did not show any false detection in the air.

V. CONCLUSION

This paper introduced a novel approach to identify a contact for a multibody robotic system. Unlike traditional approaches which use a state observer or heuristic methods, the proposed method uses a probabilistic approach. Consequently, it can fuse multiple sensor measurements in estimation. The measurement models show that not any single measure can detect a contact accurately and robustly. Only the combined information provides a reliable contact state estimate. The proposed method was verified both in simulation and with a real hardware. The proposed contact detection strategy was reliable in both cases. Even though this paper describes the basic version of the approach, the proposed strategy can also include additional sensors (e.g. IMU on leg links) thanks to its probabilistic formulation.

REFERENCES

- [1] M. Hutter, C. Gehring, M. Hopflinger, M. Bloesch, and R. Siegwart, "Toward combining speed, efficiency, versatility, and robustness in an autonomous quadruped," *IEEE Transactions on Robotics*, vol. 30, pp. 1427–1440, 2014.
- [2] M. Hutter, C. Gehring, D. Jud, A. Lauber, C. D. Bellicoso, V. Tsounis, J. Hwangbo, P. Fankhauser, M. Bloesch, R. Diethelm, and S. Bachmann, "AnyMal - a highly mobile and dynamic quadrupedal robot," *submitted to IEEE/RSJ International Conference on Intelligent Robots and Systems (IROS)*, 2016.
- [3] D. J. Hyun, S. Seok, J. Lee, and S. Kim, "High speed trot-running: Implementation of a hierarchical controller using proprioceptive impedance control on the MIT cheetah," *The International Journal of Robotics Research*, vol. 33, pp. 1417–1445, 2014.
- [4] M. Focchi, V. Barasuol, I. Havoutis, J. Buchli, C. Semini, and D. G. Caldwell, "Local reflex generation for obstacle negotiation in quadrupedal locomotion," *Nature-Inspired Mobile Robotics*, pp. 443–450, 2013. [Online]. Available: http://www.worldscientific.com/doi/abs/10.1142/9789814525534_{_}0056
- [5] A. De Luca, A. Albu-Schäffer, S. Haddadin, and G. Hirzinger, "Collision detection and safe reaction with the dlr-iii lightweight manipulator arm," *IEEE International Conference on Intelligent Robots and Systems*, pp. 1623–1630, 2006.
- [6] S. Haddadin, A. Albu-Schäffer, A. De Luca, and G. Hirzinger, "Collision detection and reaction: A contribution to safe physical human-robot interaction," *2008 IEEE/RSJ International Conference on Intelligent Robots and Systems, IROS*, pp. 3356–3363, 2008.
- [7] M. Bloesch, M. Hutter, M. a. Hoepflinger, S. Leutenegger, C. Gehring, C. D. Remy, and R. Siegwart, "State estimation for legged robots - consistent fusion of leg kinematics and imu," *Proceedings of Robotics: Science and Systems*, 2012.
- [8] G. Pratt and M. Williamson, "Series elastic actuators," in *Proceedings 1995 IEEE/RSJ International Conference on Intelligent Robots and Systems. Human Robot Interaction and Cooperative Robots*, vol. 1, pp. 399–406.